



## CASE REPORT

# CD137 deficiency because of two novel biallelic *TNFRSF9* mutations in a patient presenting with severe EBV-associated lymphoproliferative disease

Kefeng Shen<sup>a</sup> , Jiachen Wang<sup>a</sup>, Kuangguo Zhou, Wei Mu, Meilan Zhang, Xinyue Deng, Haodong Cai, Wei Zhang, Wei Huang & Min Xiao 

Department of Hematology, Tongji Hospital, Tongji Medical College, Huazhong University of Science and Technology, Wuhan, China

**Correspondence**

M Xiao and W Huang, Department of Hematology, Tongji Hospital, Tongji Medical College, Huazhong University of Science and Technology, No. 1095 Jie Fang Avenue, Hankou, Wuhan 430030, China.  
E-mail: [xiaomin@tjh.tjmu.edu.cn](mailto:xiaomin@tjh.tjmu.edu.cn) and [2896607051@qq.com](mailto:2896607051@qq.com)

<sup>a</sup>Equal contributors.

Received 1 October 2022;  
Revised 5 April 2023;  
Accepted 6 April 2023

doi: 10.1002/cti2.1448

*Clinical & Translational Immunology*  
2023; 12: e1448

**Abstract**

**Objectives.** Increasing evidence indicates that some germline genetic mutations that impair pathways required for robust host immune surveillance against EBV infection may result in an extremely high susceptibility to EBV-associated lymphoproliferative disease (EBV<sup>+</sup> LPD). *TNFRSF9* encodes a vital costimulatory molecule that enhances CD8<sup>+</sup> T-cell proliferation, survival and cytolytic activity. To date, no relevant case resulting from *TNFRSF9* heterozygous mutations has been identified. **Methods.** Here, we report the first case of CD137 deficiency caused by two novel biallelic heterozygous *TNFRSF9* mutations [NM\_001561.5: c.208 + 1→AT and c.452C>A (p.T151K)] in a patient presenting with severe EBV<sup>+</sup> LPD. Immunophenotyping and *in vitro* assays of lymphocyte function and NK cell activity were performed. **Results.** Biallelic *TNFRSF9* mutations resulted in markedly reduced or abrogated expression of CD137 on activated T, B and NK cells. CD8<sup>+</sup> T cells from the patient had impaired activation, reduced expression/release of interferon- $\gamma$  (IFN- $\gamma$ ), tumor necrosis factor- $\alpha$  (TNF- $\alpha$ ), perforin and granzyme B, and diminished cytotoxic activity. Functional experiments identified both variations were hypomorphic mutations and played a contributing role in CD137 deficiency and the development of EBV<sup>+</sup> LPD. **Conclusion.** Our study expands the genetic spectrum and clinical phenotype of patients with CD137 deficiency and provides additional evidence that the *TNFRSF9* gene plays a critical role in host immune responses to EBV infection.

**Keywords:** EBV infection, EBV-associated lymphoproliferative disease, germline genetic mutation, primary immunodeficiency, *TNFRSF9*

**INTRODUCTION**

Epstein–Barr virus (EBV) is a ubiquitous gamma herpesvirus that infects > 90% of the population worldwide; infection with the virus is lifelong.

Epstein–Barr virus predominantly infects B cells but can also infect T and NK cells.<sup>1</sup> Primary EBV infections occur asymptotically in early childhood or cause only a brief, mild illness in infected people. A small number of people may develop benign, self-

limiting infectious mononucleosis (IM), and a rare subset may develop the more serious or even life-threatening EBV-associated lymphoproliferative disease (EBV<sup>+</sup> LPD).<sup>2,3</sup>

EBV-associated lymphoproliferative disease comprises a heterogeneous group of diseases characterised by the proliferation and/or transformation of EBV-infected B, T or NK cells, ranging from lymphoproliferation with no or minimal malignant potential to aggressive lymphoma.<sup>4</sup> Increasing evidence indicates that some germline genetic mutations (e.g. in *SH2D1A*, *ITK*, *MAGT1*, *CTPS1*, *RASGRP1*, *CD27*, *CD70*, *PIK3CD*, *CORO1A* and *CARMIL2*) that impair pathways required for robust host immune surveillance against EBV infection may result in an extremely high susceptibility to EBV<sup>+</sup> LPD.<sup>5</sup> Our previous studies also provided further insights into understanding a spectrum of EBV<sup>+</sup> T/NK-LPDs with respect to genetic defects associated with lymphocyte cytotoxicity.<sup>6,7</sup> The potential genetic aetiologies may be generally summarised as two points: (1) defective activation/proliferation of EBV-specific CD8<sup>+</sup> T cells results from genetic lesions involved in T-cell activation, DNA metabolism or co-stimulatory pathways, leading to damaged elimination of proliferating EBV-infected B cells and the occurrence of lymphoproliferative disease; and (2) impaired cytotoxicity of CD8<sup>+</sup> T and/or NK cells against EBV-infected B cells caused by genetic defects related to lymphocyte cytotoxic pathway, resulting in protracted T-cell expansion/activation and persistence of EBV-infected cells.<sup>8,9</sup>

*TNFRSF9* (also referred to as CD137 and 4-1BB) gene encodes a vital costimulatory molecule that enhances CD8<sup>+</sup> T-cell proliferation, survival and cytolytic activity. To date, no relevant case resulting from *TNFRSF9* heterozygous mutations has been identified. Here, we report the first case of CD137 deficiency caused by two novel biallelic heterozygous *TNFRSF9* mutations in a patient presenting with severe EBV<sup>+</sup> LPD. Our results expand the genetic spectrum and clinical phenotype of patients with CD137 deficiency and provide additional evidence that the CD137 pathway is of vital importance in anti-EBV immunity.

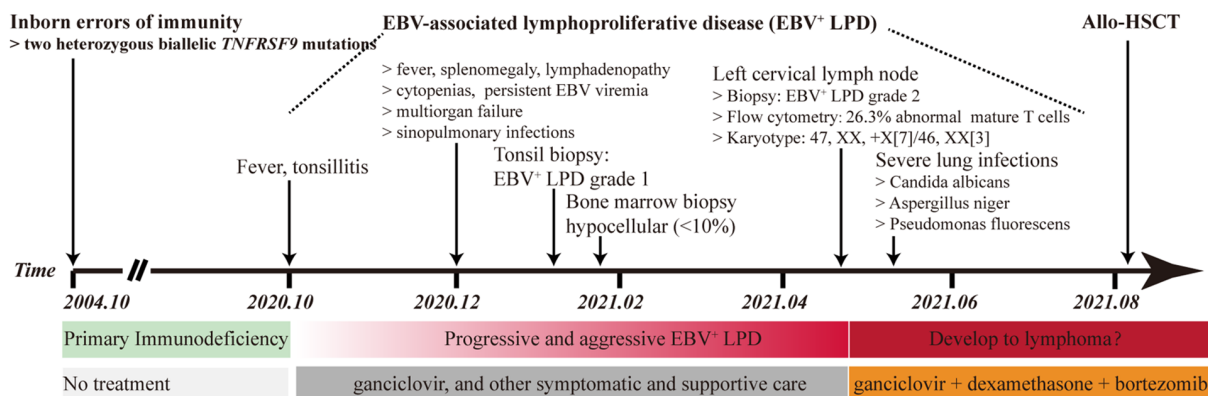
## RESULTS

### Case report

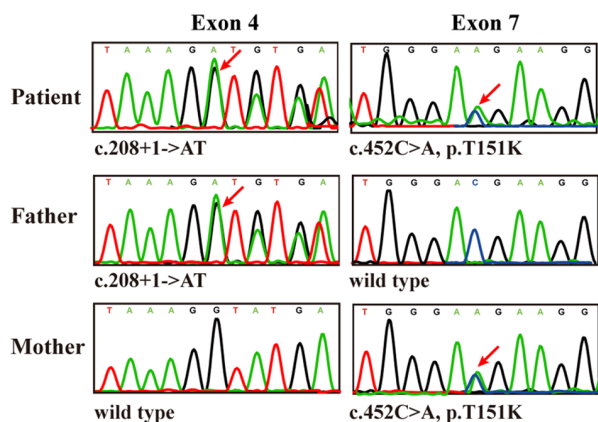
In December 2020, a 16-year-old adolescent female patient with no relevant personal nor

familial medical history was admitted to our hospital and presented with a 2-month history of intermittent low-grade fever and tonsillitis. She experienced the typical signs and symptoms of EBV<sup>+</sup> LPD, including prolonged fever, splenomegaly, lymphadenopathy, cytopenias, EBV viremia, multiorgan failure and sinopulmonary infections. Anti-EBV antibodies tests revealed high antibody levels of antiviral early antigen (EA)-IgG, antiviral capsid antigen (VCA)-IgG and antiviral nuclear antigen (NA)-IgG, and these EBV serological findings were suggestive of chronic active Epstein-Barr virus (CAEBV) infection (Supplementary figure 1b). Furthermore, monitoring of EBV DNA loads in plasma and peripheral blood mononuclear cells (PBMCs) both showed persistently high EBV DNA levels over 4 months (Figure 1c). The phenotypes of EBV-infected cells were determined using EBV sorting PCR at two different time points, demonstrating that EBV was predominantly enriched in T cells and B cells (Supplementary figure 1c). In January 2021, an excisional tonsil biopsy revealed pathological findings and histologic grading of EBV<sup>+</sup> LPD grade 1 (Supplementary figure 1d). Thus, she fulfilled the established diagnostic criteria for a probable EBV<sup>+</sup> LPD diagnosis. Treatment involving the administration of combined antifungal and antibiotic therapy as well as antiviral treatment with intravenous ganciclovir had moderate efficacy, and the disease progressively worsened. Three months later, an additional excisional biopsy of the left cervical lymph node revealed EBV<sup>+</sup> LPD grade 2 (Supplementary figure 1d). <sup>18</sup>F-fluorodeoxyglucose (FDG) PET/CT imaging in December 2020 and April 2021 indicated a rapid disease progression (Supplementary figure 1a). Subsequently, multiparametric flow cytometry analysis of the left cervical lymph node identified abnormal mature T cells of uncertain nature (reactive T-cell proliferation or malignant T-cell lymphoma) with a percentage of 26.3% in total nucleated cells (Supplementary figure 5a), and cytogenetic analysis revealed an abnormal karyotype of 47, XX,+X [7]/46,XX [3] (Supplementary figure 5b). These findings suggested that the disease potentially transformed into a malignant lymphoma with a high level of clinical suspicion. In addition, the patient developed severe lung infections caused by a combination of bacterial, fungal and viral pathogens, including *Pseudomonas fluorescens*, *Candida albicans*,

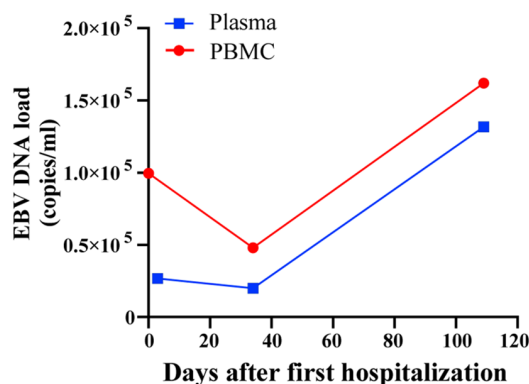
**(a) Patient timeline**



**(b) Sanger validation (*TNFRSF9*, NM\_001561.5)**



**(c) EBV DNA load in plasma and PBMC**



**(d) Diagram of gene structure and pathogenic mutations**

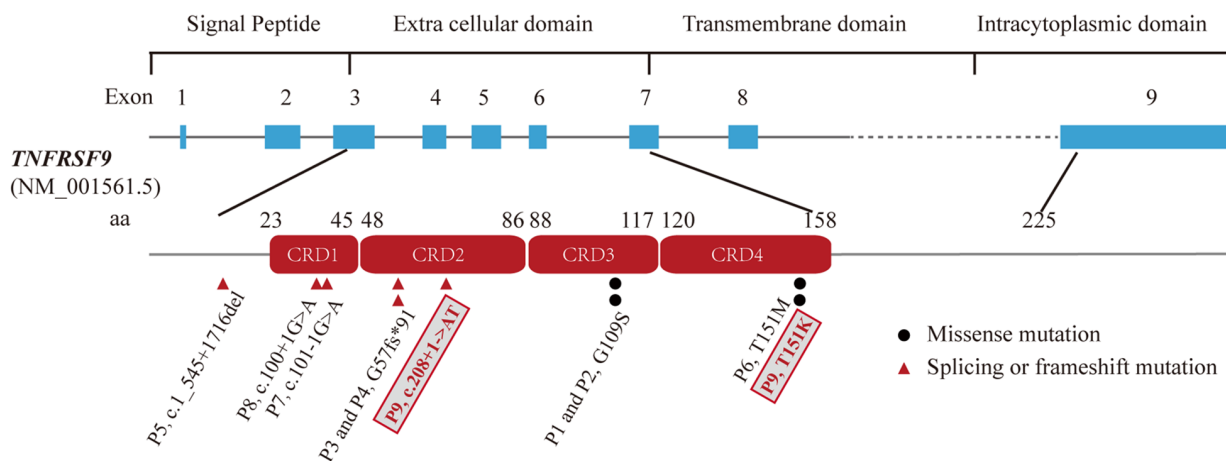


**Figure 1.** A brief summary of the medical history, laboratory evaluation and genetic presentations of the patient with EBV<sup>+</sup> LPD. **(a)** Patient timeline of key clinical events and laboratory test results. **(b)** Sanger sequencing chromatograms were performed on the buccal swab samples, confirming the *TNFRSF9* mutations in the patient's family. **(c)** Sequential EBV DNA loads in the plasma and PBMCs of the patient. The cut-off value of positive EBV load was  $5.0 \times 10^2$  copies mL<sup>-1</sup>. **(d)** A schematic illustration of *TNFRSF9* showing its domains and localisation of identified mutations. All 8 mutations affect the extracellular domain and result in loss of function. P1-P8 represents previously reported patients listed in Table 1. P9 represents our patient.

*Aspergillus niger* and EBV. Considering the extremely poor prognosis, she was treated with an adjusted antiviral schedule of high-dose ganciclovir and dexamethasone combined with bortezomib to temporarily reduce the systemic toxicity associated with EBV<sup>+</sup> T-cell infiltration and allow the patient time to receive allogeneic haematopoietic stem cell transplantation (allo-HSCT) in another hospital. More detailed patient information can be found in Figure 1a.

### Biallelic *TNFRSF9* mutations in the patient abolish CD137 expression

Because of the patient's clinical features and high clinical suspicion of a primary immune deficiency, whole-exome sequencing (WES) analysis of the initial bone marrow sample was performed to elucidate the disease aetiology. Two novel compound heterozygous mutations were identified in the *TNFRSF9* gene and confirmed by Sanger sequencing, and both healthy parents were heterozygous carriers (Figure 1b). The first was a *TNFRSF9* splicing mutation (NM\_001561.5: c.208 + 1→AT) that was inherited from her father and the second was a missense mutation (NM\_001561.5: c.452C>A, p. T151K) inherited from her mother. Furthermore, Supplementary table 1 listed all the variants of the patient discovered by WES with a minor allele frequency of < 0.001 in gnomAD database. No other pathogenic/likely pathogenic variants were detected in genes known to be associated with predisposition to EBV infection.

To investigate whether our patient's compound heterozygous *TNFRSF9* mutations (c.208 + 1→AT and p.T151K) resulted in CD137 deficiency, we next evaluated the effect of the two variations on CD137 expression of blood samples from the patient, her parents and three age- and sex-matched healthy donors (HDs) by flow cytometry. In the compound heterozygous patient, biallelic *TNFRSF9* mutations resulted in markedly reduced or abrogated expression of CD137 on activated CD4<sup>+</sup> and CD8<sup>+</sup> T, B and NK cells, indicating a loss-of-function phenotype (Figure 2a and Supplementary figure 3a). Accordingly, the cells from the heterozygous parents demonstrated a partial or moderate reduction in CD137 expression compared with HDs, suggesting that CD137 deficiency was mainly determined in a gene dose-dependent manner (biallelic inactivation of *TNFRSF9* gene was more deleterious than

monoallelic inactivation) (Figure 2a and Supplementary figure 3a). Interestingly, the father's CD137 expression reduction tended to be more serious than that of the mother, one possible reason was that the pathogenicity grade of the splicing mutation might be stronger than the missense mutation according to ACMG guidelines (Supplementary figure 3a).

### Impaired activation, reduced production of cytokine and cytolytic granules, and defective cytotoxicity of patient's CD8<sup>+</sup> T cells

Early studies consistently reported that CD137 promotes CD8<sup>+</sup> T-cell activation, survival, cytokine secretion and cytotoxic activity.<sup>10–12</sup> Thus, we performed some *in vitro* assays of T-cell function and NK cell activity in our study. A flow cytometry-based assay was utilised to assess CD4<sup>+</sup> and CD8<sup>+</sup> T-cell activation induced through CD3 costimulation by detecting the expression of early activation marker CD69. CD8<sup>+</sup> T cells from the compound heterozygous patient had extremely impaired activation, while the heterozygous parents showed a slightly defective CD8<sup>+</sup> T-cell activation compared with HDs, showing a dose-dependent defect (Figure 2b and Supplementary figure 3b). Intriguingly, CD4<sup>+</sup> T cells from the patient had an abrogated CD137 expression but did not demonstrate a defective activation, suggesting that it might be compensated in the presence of other costimulatory molecules or alternative pathways (Supplementary figure 2a).

Robust cytotoxicity and cytokine production are of vital importance for T-cell function, making cytotoxic T lymphocytes able to efficiently eliminate EBV-infected cells. Degranulation, an indispensable prerequisite for perforin/granzyme-mediated killing, is the fundamental mechanism by which CD8<sup>+</sup> T or NK cell-mediated cytolytic activity. Correspondingly, we examined the production of T-cell cytokines (IL-2, IFN- $\gamma$  and TNF- $\alpha$ ) and assessed the expression of cytotoxic effector molecules (perforin and granzyme B) and degranulation marker CD107a after various strong antigenic stimulation. The patient's CD8<sup>+</sup> T cells had significantly reduced expression/release of IFN- $\gamma$ , TNF- $\alpha$ , perforin and granzyme B compared with HDs (Figure 2c and d). We evaluated the surface expression of CD107a, reflecting the exocytosis of lytic granules and being applied as a good marker

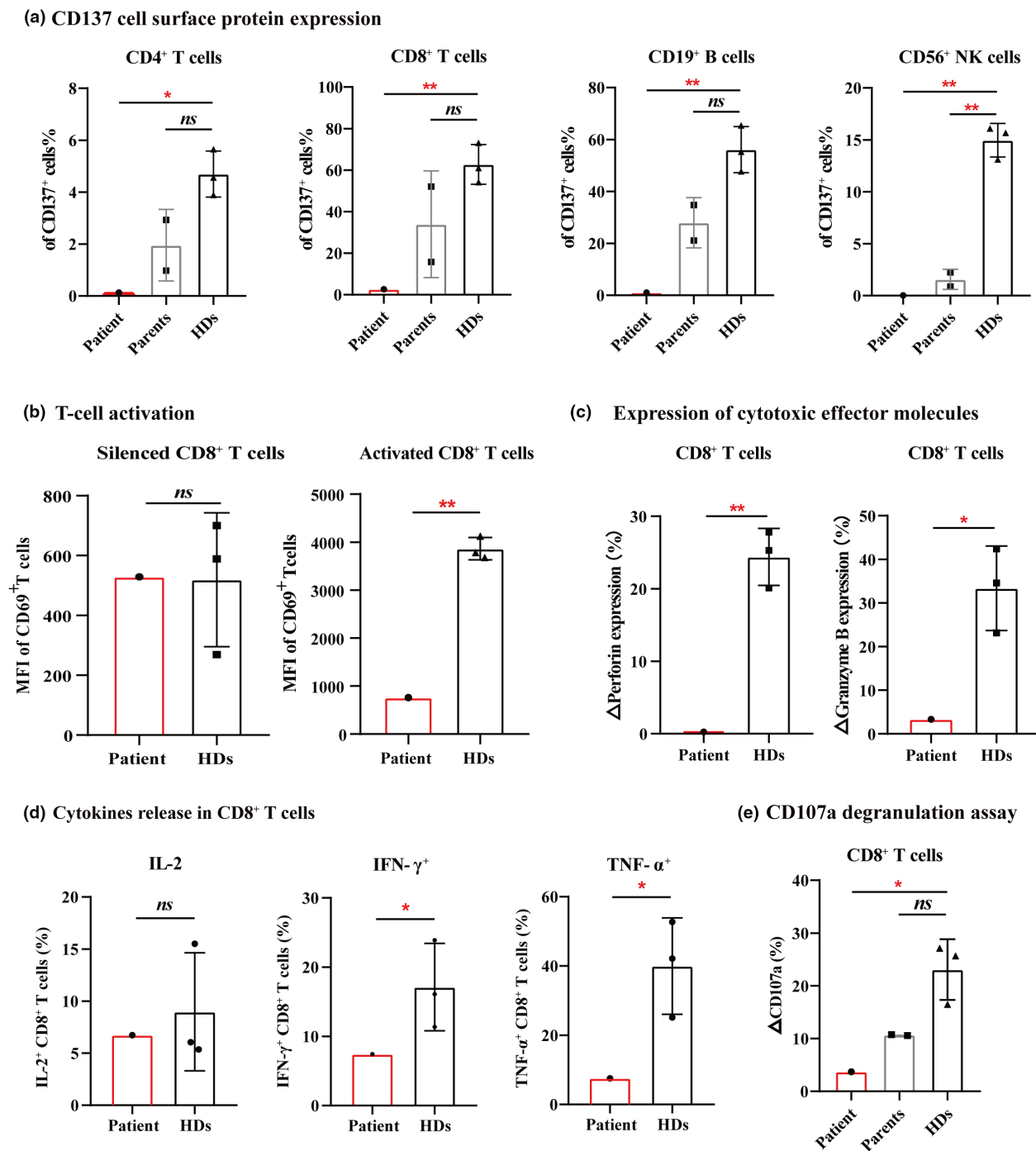


**Figure 2.** Immunological and functional phenotypes of the patient with EBV<sup>+</sup> LPD. **(a)** CD137 protein expression in activated CD4<sup>+</sup> and CD8<sup>+</sup> T cells, activated CD19<sup>+</sup> B cells and activated CD56<sup>+</sup> NK cells in the patient, parents and HDs, demonstrating complete loss or markedly reduced expression in the patient cells, as measured by flow cytometry. **(b)** Mean fluorescence intensity (MFI) on CD69<sup>+</sup> T cells after 4 days of CD3 costimulation in the patient and HDs, demonstrating a CD8<sup>+</sup> T-cell activation defect of the patient. **(c)** Representative fluorescence-activated cell-sorting analysis of perforin- and granzyme B-positive cells in CD8<sup>+</sup> T cells from the patient and HDs. **(d)** Fluorescence-activated quantitative analysis of IL-2, IFN- $\gamma$  and TNF- $\alpha$  in CD8<sup>+</sup> T cells after stimulation with leukocyte activation cocktail (BD, Golgiplug, 550 583), demonstrating a reduced release of IFN- $\gamma$  and TNF- $\alpha$  in CD8<sup>+</sup> T cells of the patient. **(e)** Degranulation was measured in CD8<sup>+</sup> T cells stimulated with CD3/CD28 through CD107a expression by flow cytometry, demonstrating a CD8<sup>+</sup> T-cell degranulation defect in the patient. All assays of the patient, parents and HDs ( $n = 3$ ) were performed in two independent experiments. All columns and bars represent means  $\pm$  standard deviations (SDs). \* $P < 0.05$ , \*\* $P < 0.01$ . ns, Not significant.



for the degranulation of activated CD8<sup>+</sup> T and NK cells. CD107a assays revealed the CD8<sup>+</sup> T cells of the patient with an obvious degranulation defect (< 5%) (Figure 2e).

Subsequently, we performed similar functional assays with NK cells. We found that activated NK cells from the patient showed robust expression/release of perforin and granzyme B, normal levels of cytotoxicity against K562 target cells and unaffected CD107a degranulation, revealing the patient had a normal NK cell function (Supplementary figure 2c–e).

## DISCUSSION

We have identified herein an immunodeficient patient of CD137 deficiency, resulting from two novel biallelic mutations (c.208 + 1→AT and p.T151K) in the *TNFRSF9* gene, characterised by a progressive/aggressive EBV-induced lymphoproliferative disease with features of recurrent infections and uncontrolled CAEBV. A comprehensive *in silico* analysis of the functional and structural impact was then performed. Both the two variants were located in the highly conserved Cysteine-rich domain (CRD) and predicted to be deleterious by the Human Splicing Finder (<http://www.umd.be/HSF/>) or PolyPhen-2, SIFT and CADD algorithms, and absent in the current gnomAD, ExAC and 1000G databases, and both belonged to pathogenic variants according to the ACMG guideline.<sup>13</sup> Interestingly, the p.T151K mutation was at the exact same position but with a different nucleotide substitution as the variant p.T151M of Somekh I *et al.*'s study.<sup>12</sup> In addition, we performed several *in vitro* functional assays of T and/or NK cells derived from the patient, parents and healthy donors to assess cytokine production, lytic granules release and cytotoxicity in our study. Functional analysis indicated that CD137 deficiency mainly impairs the activation and cytotoxic function of CD8<sup>+</sup> T cells in a gene dose-dependent manner, while NK cells may not be involved.

In recent years, next-generation sequencing (NGS) approaches have been increasingly utilised in clinical practice to elucidate the molecular aetiology of primary immunodeficiency diseases (PID), improving our understanding and knowledge of this genetically heterogeneous disease. Previous studies of PID patients with common clinical features of chronic EBV viremia and/or EBV-driven disease (e.g. HLH,

lymphoproliferation, and lymphoma) have resulted in an expanding list of causal genes involved in innate and adaptive immunity against EBV infection. In 2019, eight patients carrying six distinct homozygous mutations in the *TNFRSF9* gene linked to combined immune deficiency were first reported by Alosaimi MF *et al.*, Rodriguez R *et al.* and Somekh I *et al.*, and all eight patients developed EBV<sup>+</sup> LPD to some extent (see Table 1 and Figure 1d for more details).<sup>10–12</sup> They found that (1) homozygous *TNFRSF9* mutations reduce or abolish the surface expression of CD137 on activated T, B and NK cells, resulting in dysfunction of affected CD8<sup>+</sup> T cells characterised by impaired activation and proliferation, reduced production of IFN- $\gamma$  and perforin, restricted TCR repertoire diversity and diminished cytotoxic activity in response to EBV-infected B cells. Activated CD8<sup>+</sup> T cells from the patients also had decreased mitochondrial activity and biogenesis, which likely contributed to the defective CD8<sup>+</sup> T cell cytotoxicity. (2) This effect can also disrupt B-cell function with impaired activation, proliferation and class switch recombination (CSR).<sup>12</sup> However, NK-cell degranulation and TCR-signalling pathways were intact in the patients, suggesting they were not directly affected by CD137. Together, all these factors may contribute to the defective expansion and cytotoxicity of EBV-specific CD8<sup>+</sup> T cells, leading to impaired elimination of EBV-infected B cells and the occurrence of EBV<sup>+</sup> LPD. Interestingly, four siblings of the eight patients harbouring identical homozygous *TNFRSF9* mutations were mildly symptomatic or clinically asymptomatic, suggesting an incomplete penetrance in CD137 deficiency.

In this study, we get some similar results consistent with the previous three studies. Biallelic *TNFRSF9* mutations of the patient resulted in markedly reduced or abrogated expression of CD137 on activated T, B and NK cells. CD8<sup>+</sup> T cells from the affected patient had impaired activation, reduced expression/release of IFN- $\gamma$ , TNF- $\alpha$ , perforin and granzyme B and diminished cytotoxic activity. Functional experiments suggested that CD137 deficiency had no or minor effects on the release of cytotoxic molecules and the cytotoxicity of activated NK cells. In addition, our results also provide some new insights. (1) First, no relevant case resulting from *TNFRSF9* heterozygous mutations has been identified to date, and whether two compound-heterozygous mutations in *TNFRSF9* can result in a similar immunodeficiency case has not been

**Table 1.** Genetics, clinical manifestations and mechanisms of CD137 deficiency patients

Patient	Type of Mutation	Clinical features	Treatment	Mechanisms
P1 (Ref10)	<i>TNFRSF9</i> (G109S, Homo)	Saudi, female, parental consanguineous marriages. Age of onset, 3 years. Recurrent sinopulmonary infections, lymphadenopathy, persistent EBV viremia, EBV <sup>+</sup> B-LPD, hypogammaglobulinemia, HLH. Alive now.	IVIg, rituximab, Allo-HSCT.	↓proliferation/IFN- $\gamma$ and perforin expression/cytotoxic activity of CD8 <sup>+</sup> T cells; ↓mitochondrial mass/membrane potential/function of CD8 <sup>+</sup> T cells.
P2 (Ref10)	<i>TNFRSF9</i> (G109S, Homo)	Saudi, male, parental consanguineous marriages. Age of onset, 6 years. Recurrent sinopulmonary infections, lymphadenopathy, splenomegaly, EBV viremia, EBV <sup>+</sup> Hodgkin disease, progression to EBV <sup>+</sup> DLBCL. Alive now.	Chemotherapy for lymphoma, IVIg for infections.	
P3 (Ref11)	<i>TNFRSF9</i> (G57fs*91, Homo) and <i>PIK3CD</i> (R821H, Homo)	Pakistani, male, parental consanguineous marriages. Age of onset, 3 months. Recurrent respiratory and skin infections, hepatosplenomegaly, lymphadenopathy, EBV <sup>+</sup> T-LPD, fatal T-cell type CAEBV, HLH. Died of fatal HLH	Antibiotic intravenous infusion, anti-CD20 antibody.	impaired T-cell expansion.
P4 (Ref11)	<i>TNFRSF9</i> (G57fs*91, Homo)	Sibling of P3, Pakistani, female, parental consanguineous marriages. Age of onset, 6 years. Asymptomatic up to now, persistent EBV viremia and circulating EBV-infected T cells. Alive now.	not available	
P5 (Ref12)	<i>TNFRSF9</i> (c.1_545 + 1716del, Homo)	Turkish, male, parental consanguineous marriages. Age of onset, 2 years. EBV <sup>+</sup> Burkitt lymphoma, recurrent ear infections, EBV viremia, hepatosplenomegaly, hypogammaglobulinemia. Alive now.	Chemotherapy for lymphoma, IVIg, antibiotic therapy.	↓impaired T-cell survival, proliferation and cytotoxicity; ↓TCR repertoire diversity; ↓activation, affinity maturation, proliferation and class switch recombination of B cells.
P6 (Ref12)	<i>TNFRSF9</i> (T151M, Homo)	Palestinian, male, parental consanguineous marriages. Age of onset, 3 years. Recurrent pneumonia, hepatosplenomegaly, lymphadenopathy, autoimmunity, ALPS-like disease manifestations, EBV <sup>+</sup> T-LPD. Alive now.	Sirolimus and glucocorticoids, cellcept therapy, antibiotic prophylaxis.	
P7 (Ref12)	<i>TNFRSF9</i> (c.101-1G>A, Homo)	Turkish, male, parental consanguineous marriages. Age of onset, 6 years. Recurrent infections of bacterial and viral origin, hepatosplenomegaly, lymphadenopathy, atopic dermatitis and xerosis, hypergammaglobulinemia, autoimmunity, EBV <sup>+</sup> Hodgkin lymphoma. Alive now.	IVIg, chemotherapy, amoxicillin prophylaxis.	
P8 (Ref12)	<i>TNFRSF9</i> (c.100 + 1G>A, Homo)	Colombian, male. Age of onset, 8 years. Recurrent sinopulmonary infections, EBV viremia, hepatosplenomegaly, hypogammaglobulinemia, diagnosis of CVID, granulomatous pleuropneumonia. Alive now.	Subcutaneous immunoglobulin infusion	
P9	<i>TNFRSF9</i> (c.208 + 1→AT, Heter) and (T151K, Heter)	Chinese, female. Age of onset, 16 years. Recurrent sinopulmonary infections, fever, splenomegaly, lymphadenopathy, cytopenia, persistent EBV viremia, multiorgan failure, CAEBV, EBV <sup>+</sup> LPD. Alive now.	Intravenous ganciclovir, antifungal and antibiotic therapy, IVIg, bortezomib.	↓Activation, cytokines (IFN- $\gamma$ , TNF- $\alpha$ ), cytotoxic activity (perforin, granzyme B, degranulation) of CD8 <sup>+</sup> T cells.

ALPS, Autoimmune lymphoproliferative syndrome; CVID, Common variable immune deficiency; DLBCL, Diffuse large B-cell lymphoma; Heter, heterozygous; HLH, Hemophagocytic lymphohistiocytosis; Homo, homozygous; IVIg, Intravenous immunoglobulin; Ref, Reference.

demonstrated. Thus, our results may complement previous studies. (2) Second, our patient's age of clinical onset was greater (16 years vs 0.25–8 years)

than that of the eight previously reported patients. We currently do not know the reason, a possible explanation may be relevant to the compound-

heterozygous mutation state resulting in delayed disease onset. (3) Last, our patient was born to a nonconsanguineous family and might be rarer than the previous eight patients, of whom seven were from consanguineous kindreds and one had no known consanguinity. Regretfully, functional assays of our study mainly focussed on T-cell function and NK-cell cytotoxicity because of the limited availability of blood samples from the patient; thus, further studies on B-cell function were not completed.

In summary, we identified the first case of CD137 deficiency caused by two novel biallelic heterozygous *TNFRSF9* mutations in a patient presenting with severe EBV<sup>+</sup> LPD. Of note, the quantity and quality of CD8<sup>+</sup> T cells are crucial for controlling EBV infection.<sup>14,15</sup> CD137 deficiency impairs the expansion and cytotoxicity of CD8<sup>+</sup> T cells, thus resulting in a predisposition to EBV<sup>+</sup> LPD. Our study expands the genetic spectrum and clinical phenotype of patients with CD137 deficiency and provides additional evidence that the *TNFRSF9* gene plays a critical role in host immune responses to EBV infection.

## METHODS

### Whole-exome sequencing (WES)

For WES on the initial bone marrow sample, the library was constructed using Fast Library Prep Kit, and then the whole exons were captured with ALEXOME Enrichment Kit V1 (iGeneTech). Sequencing was performed on Illumina platform (Illumina) with 150-base-paired-end reads. Raw reads were filtered to remove low-quality reads using FastQC. Then, clean reads were mapped to the reference genome GRCh37 using BWA. After removing duplications, SNV and InDel were called and annotated using GATK. Describing Sequence Variants Using HGVS Nomenclature.

### Expansion of T cells and NK cells

Fresh whole-blood samples were collected in EDTA-containing vials and sent to the laboratory at room temperature. Peripheral blood mononuclear cells (PBMCs) were isolated by standard Ficoll–Hypaque gradient centrifugation. T cells were expanded by stimulation of the PBMCs with Dynabeads™ Human T-Activator CD3/CD28 (Gibco) at a 1:5 ratio in CTS™ OpTmizer™ medium (Gibco) containing 10% foetal bovine serum (FBS, Gibco), 2 mM l-glutamine (Gibco, Grand Island, NY, USA) and 200 IU mL<sup>-1</sup> rhIL-2 (PeproTech, Rocky Hill, NJ, USA). NK cells were expanded by stimulation of the PBMCs with 100 IU mL<sup>-1</sup> rhIL-2 (PeproTech).

### Flow cytometry and antibodies

For analysis of cell surface markers, PBMCs were used as starting material. Cells were washed twice in FACS buffer (PBS with 5% FBS) and resuspended in 100 µL of FACS buffer with

antibodies for 30 min on ice. Cells were washed twice in FACS buffer and resuspended in 300 µL of FACS buffer. Data were acquired on a FACS Calibur (Becton Dickinson) and analysed using the FlowJo software (TreeStar).

### CD137 expression

CD137 expression on T cells was measured upon 48-h stimulation of PBMCs with Dynabeads™ Human T-Activator CD3/CD28 (Gibco) at a 1:5 ratio. Cells were stained with anti-CD137-APC (4B4-1, BD Biosciences, San Diego, USA), anti-CD3-PacB (clone SK7, BioLegend), anti-CD4-PE (SK3, BioLegend) and anti-CD8-PE-Cy7 (SK1, BioLegend, San Diego, USA). The expression on activated NK cells and B cells were measured upon 48-h stimulation of PBMCs with IL-2 600 U mL<sup>-1</sup> (PeproTech). Peripheral blood mononuclear cells were stained with anti-CD137-APC (4B4-1, BD Biosciences), anti-CD3-PacB (SK7, BioLegend), anti-CD56-PE (B159, BD Biosciences) and anti-CD19-BV605 (SJ25C1, BD Biosciences).

### T-cell activation

Flow-cytometric expression of CD69<sup>+</sup> was depicted in patients and HDs upon 96-h stimulation with Dynabeads™ Human T-Activator CD3/CD28 (Gibco) at a 1:5 ratio. Cells were stained with anti-CD69-PE-Cy7 (FN50, BioLegend), anti-CD3-FITC (clone HIT3α, BioLegend), anti-CD4-APC (OKT4, BioLegend) and anti-CD8-BV650 (RPA-T8, BD Biosciences).

### Intracellular cytokine staining

Peripheral blood mononuclear cells ( $5 \times 10^5$ ) were incubated with BD Leukocyte Activation Cocktail (Ionomycin, Brefeldin A and phorbol myristic acetate (PMA)) in the presence of BD GolgiStop for 4 h and then incubated with anti-CD3-PacB (clone SK7, BioLegend), anti-CD4-PE (SK3, BioLegend) and anti-CD8-PE-Cy7 (SK1, BioLegend). Then, cells were fixed and permeabilised with BD Cytofix/Cytoperm as previously described,<sup>10</sup> and intracellularly stained with anti-IL2-FITC (clone MQ1-17H12, BioLegend), anti-IFN-γ-APC (clone 4S.B3, BioLegend) and anti-TNF-α-BV655 (clone Mab11, BioLegend).

### Intracellular staining for perforin and granzyme B

For each staining,  $2 \times 10^5$  PBMCs were washed, surface stained with anti-CD3-Percp (clone SK7, BD Biosciences), anti-CD8-APC-Cy7 (clone SK1, BioLegend) and anti-CD56-APC (clone HCD56, BioLegend) in FACS buffer. For intracellular staining, cells were fixed and permeabilised with cytofix/cytoperm solution (BD Biosciences) according to the manufacturer's instructions and stained intracellularly with anti-perforin-PE (clone B-D48, BioLegend), anti-granzyme B-FITC (clone C89, BioLegend).

### CTL and NK-cell degranulation tests

NK-cell and CTL (Cytotoxic T Lymphocyte) degranulation were assessed by CD107a surface staining without medium-



cultured cells and 3 h after stimulation with K562 cells at a ratio of 1:1 as previously described.<sup>16</sup> The K562 (ATCC, CCL-243) was used as a target cell line. NK cells were cultured in medium containing 600 U mL<sup>-1</sup> IL-2 (Peprotech) for 48 h to assess degranulation of activated NK cells. CTL degranulation was evaluated in T lymphoblasts 48 h after stimulation with 1.25 mg mL<sup>-1</sup> 1- phytohemagglutinin-L (PHA-L, Vector) and 200 U mL<sup>-1</sup> IL-2 (Peprotech). CTL degranulation was calculated by the difference in median fluorescence intensity of CD107a of CTLs stimulated with CD3/CD28-coated microbeads (ThermoFisher Scientific) at a ratio of 1:10 for 3 h and medium cultured cells. Degranulation in CD8<sup>+</sup> T cells were stained with anti-CD3-FITC (clone HIT3 $\alpha$ , BioLegend), anti-CD8-PE-Cy7 (clone SK1, BioLegend) and anti-CD107a-APC (clone H4A3, BioLegend). Degranulation in NK cells was stained with anti-CD3-APC (clone HIT3 $\alpha$ , BioLegend), anti-CD56-BV421 (HCD56, BioLegend) and anti-CD107a-FITC (clone H4A3, BioLegend). The cut-off value of the normal resting NK cells  $\Delta$ CD107a is  $\geq 5\%$ , and the cut-off value of normal activated NK cells  $\Delta$ CD107a is  $\geq 40\%$ .

### NK-cell cytotoxicity test

The assay conditions were optimised by incubating EGFP-K562 (target) cells with PBMCs (effector cells) obtained from the patient, healthy donors and her parents for the NK-cell cytotoxicity assay. The test was performed as previously described.<sup>17,18</sup> Briefly, PBMCs were resuspended at  $2 \times 10^6$  mL<sup>-1</sup>, while EGFP-K562 cells were adjusted to  $2 \times 10^6$  mL<sup>-1</sup> in complete medium (1640 + 10% FBS). Effector (E) cells from PBMC and target (T) cells (100  $\mu$ L each) were mixed in a ratio of 1:1. Meanwhile, EGFP-K562 cells only were included as the background control. Then, the samples were incubated at 37°C with 5% CO<sub>2</sub> for 2 h. The optimised assay conditions were applied in the subsequent experiments. The samples were transferred into flow cytometry tubes following incubation. After removal of the culture medium by centrifugation, the cells were sequentially washed with cold phosphate buffer saline (PBS, ThermoFisher Scientific) and binding buffer (Annexin V-PE Apoptosis Detection Kit, eBioscience). Then, the cells were resuspended in 100  $\mu$ L binding buffer containing 5  $\mu$ L Annexin V-PE, gently mixed, and incubated in the dark for 15 min at room temperature. Afterward, 5  $\mu$ L PI (Annexin V-PE Apoptosis Detection Kit, eBioscience) was added before detection by flow cytometry. The proportions of cells in the EGFP-K562 gate were determined, including live, early apoptotic, late apoptotic and necrotic cells. After co-culture of effector cells with target cells, the apoptosis ratio of target cells was considered to reflect NK cell cytotoxicity. Meanwhile, EGFP-K562 cells without treatment were stained with Annexin V-Percp/PI as controls, to determine naturally occurring apoptosis. The NK cell activity (%) = apoptosis ratio of target cells in E/T co-culture – natural apoptosis ratio of target cells only. Cut-off of  $\Delta$ cytotoxicity is  $\geq 15\%$ .

### Statistical analysis

The one-sample *t*-test was applied to compare the results. Statistical evaluation of experimental data was performed

using Prism version 8 (GraphPad Software). *P*-values < 0.05 were considered statistically significant. *P*-values and statistical tests are shown in Supplementary table 3.

### ACKNOWLEDGMENTS

We thank the patient and her family for their participation in this study and all the faculty and staff at our Clinical and Laboratory Unit for clinical and technical support. We also acknowledge Perfectgen Diagnostics (Ezhou, Hubei Province, China) for assisting with the bioinformatics analysis.

### AUTHOR CONTRIBUTIONS

**Kefeng Shen:** Conceptualization; data curation; formal analysis; visualization; writing – original draft; writing – review and editing. **Jiachen Wang:** Data curation; formal analysis; methodology. **Kuangguo Zhou:** Investigation; resources. **Wei Mu:** Methodology; validation. **Meilan Zhang:** Investigation; validation. **Xinyue Deng:** Investigation; validation. **Haodong Cai:** Formal analysis; software. **Wei Zhang:** Investigation; resources. **Wei Huang:** Conceptualization; project administration; supervision. **Min Xiao:** Conceptualization; funding acquisition; project administration; resources; supervision.

### CONFLICT OF INTEREST

The authors declare no conflict of interest.

### ETHICAL APPROVAL

The study involving human participants was reviewed and approved by the Medical Ethics Committee of Tongji Hospital, Tongji Medical College, Huazhong University of Science and Technology (TJ-IRB20200706). Written informed consent was obtained from the individual for the publication of any potentially identifiable images or data included in this article.

### FUNDING INFORMATION

This work was supported by the National Natural Science Foundation of China (No.81770211 to Min Xiao).

### DATA AVAILABILITY STATEMENT

The data sets presented in this study can be found in online repositories. The names of the repository/repositories and accession number(s) can be found below: <https://www.ncbi.nlm.nih.gov/sra/?term=PRJNA881486>.

### REFERENCES

- Young LS, Rickinson AB. Epstein-Barr virus: 40 years on. *Nat Rev Cancer* 2004; **4**: 757–768.
- Luzuriaga K, Sullivan JL. Infectious mononucleosis. *N Engl J Med* 2010; **362**: 1993–2000.

3. Cohen JI, Kimura H, Nakamura S, Ko YH, Jaffe ES. Epstein-Barr virus-associated lymphoproliferative disease in non-immunocompromised hosts: a status report and summary of an international meeting, 8-9 September 2008. *Ann Oncol* 2009; **20**: 1472–1482.
4. Toner K, Bollard CM. EBV<sup>+</sup> lymphoproliferative diseases: opportunities for leveraging EBV as a therapeutic target. *Blood* 2022; **139**: 983–994.
5. Tangye SG, Latour S. Primary immunodeficiencies reveal the molecular requirements for effective host defense against EBV infection. *Blood* 2020; **135**: 644–655.
6. Guan YQ, Shen KF, Yang L *et al.* Inherited genetic susceptibility to nonimmunosuppressed Epstein-Barr virus-associated T/NK-cell lymphoproliferative diseases in Chinese patients. *Curr Med Sci* 2021; **41**: 482–490.
7. Luo H, Liu D, Liu W *et al.* Clinical and genetic characterization of Epstein-Barr virus-associated T/NK-cell lymphoproliferative diseases. *J Allergy Clin Immunol* 2023; **151**: 1096–1109.
8. Latour S, Winter S. Inherited immunodeficiencies with high predisposition to Epstein-Barr virus-driven lymphoproliferative diseases. *Front Immunol* 2018; **9**: 1103.
9. Latour S, Fischer A. Signaling pathways involved in the T-cell-mediated immunity against Epstein-Barr virus: lessons from genetic diseases. *Immunol Rev* 2019; **291**: 174–189.
10. Alosaimi MF, Hoenig M, Jaber F *et al.* Immunodeficiency and EBV-induced lymphoproliferation caused by 4-1BB deficiency. *J Allergy Clin Immunol* 2019; **144**: 574–583.e5.
11. Rodriguez R, Fournier B, Cordeiro DJ *et al.* Concomitant PIK3CD and TNFRSF9 deficiencies cause chronic active Epstein-Barr virus infection of T cells. *J Exp Med* 2019; **216**: 2800–2818.
12. Somekh I, Thian M, Medgyesi D *et al.* CD137 deficiency causes immune dysregulation with predisposition to lymphomagenesis. *Blood* 2019; **134**: 1510–1516.
13. Richards S, Aziz N, Bale S *et al.* Standards and guidelines for the interpretation of sequence variants: a joint consensus recommendation of the American College of Medical Genetics and Genomics and the Association for Molecular Pathology. *Genet Med* 2015; **17**: 405–424.
14. Tangye SG, Palendira U, Edwards ES. Human immunity against EBV-lessons from the clinic. *J Exp Med* 2017; **214**: 269–283.
15. Taylor GS, Long HM, Brooks JM, Rickinson AB, Hislop AD. The immunology of Epstein-Barr virus-induced disease. *Annu Rev Immunol* 2015; **33**: 787–821.
16. Bryceson YT, Pende D, Maul-Pavicic A *et al.* A prospective evaluation of degranulation assays in the rapid diagnosis of familial hemophagocytic syndromes. *Blood* 2012; **119**: 2754–2763.
17. Zhang J, Wang Y, Wu L *et al.* Application of an improved flow cytometry-based NK cell activity assay in adult hemophagocytic lymphohistiocytosis. *Int J Hematol* 2017; **105**: 828–834.
18. Gao L, Dang X, Huang L *et al.* Search for the potential "second-hit" mechanism underlying the onset of familial hemophagocytic lymphohistiocytosis type 2 by whole-exome sequencing analysis. *Transl Res* 2016; **170**: 26–39.

## Supporting Information

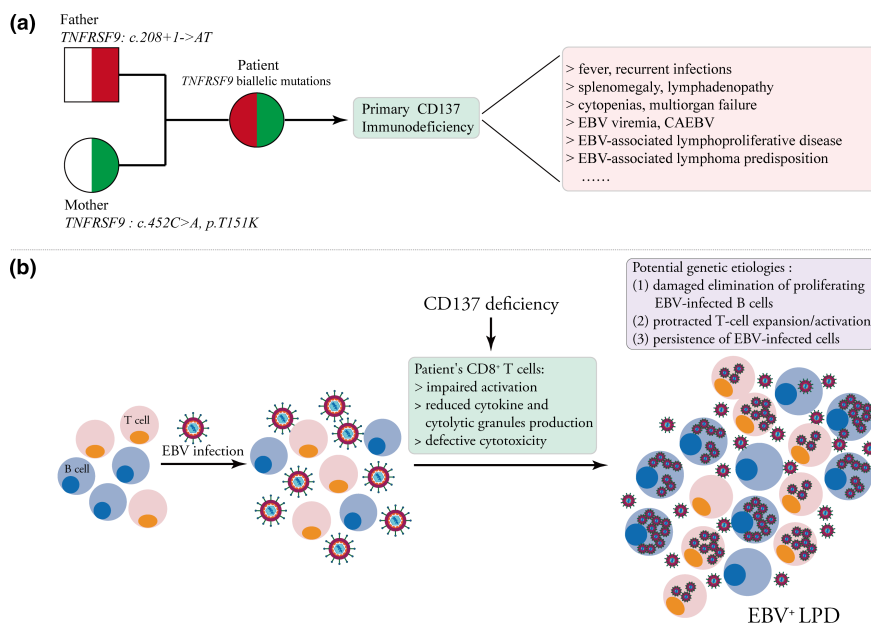
Additional supporting information may be found online in the Supporting Information section at the end of the article.



This is an open access article under the terms of the [Creative Commons Attribution-NonCommercial](#) License, which permits use, distribution and reproduction in any medium, provided the original work is properly cited and is not used for commercial purposes.

# Graphical Abstract

The contents of this page will be used as part of the graphical abstract of html only. It will not be published as part of main.



In this study, we reported the first case of CD137 deficiency caused by two novel biallelic heterozygous *TNFRSF9* mutations [NM\_001561.5: c.208 + 1->AT and c.452C>A (p.T151K)] in a patient presenting with severe EBV-associated lymphoproliferative disease. *In vitro* assays of lymphocyte function demonstrated that the patient's CD8<sup>+</sup> T cells had impaired activation, reduced production of cytokine and cytolytic granules, and defective cytotoxicity. Our results expand the genetic spectrum and clinical phenotype of patients with CD137 deficiency and provide additional evidence that the CD137 pathway is of vital importance in anti-EBV immunity.